

Gravitational Waves Induced by Scalar Perturbations during a Gradual Transition from an Early Matter Era to the Radiation Era

Keisuke Inomata^{a,b} Kazunori Kohri^{c,d} Tomohiro Nakama^e Takahiro Terada^c

^aICRR, The University of Tokyo, Kashiwa, Chiba 277-8582, Japan

^bKavli IPMU (WPI), UTIAS, The University of Tokyo, Kashiwa, Chiba 277-8583, Japan

^cTheory Center, IPNS, KEK, 1-1 Oho, Tsukuba, Ibaraki 305-0801, Japan

^dThe Graduate University for Advanced Studies (SOKENDAI), 1-1 Oho, Tsukuba, Ibaraki 305-0801, Japan

^eInstitute for Advanced Study, The Hong Kong University of Science and Technology, Clear Water Bay, Kowloon, Hong Kong

Abstract. We revisit the effects of an early matter-dominated era on gravitational waves induced by scalar perturbations. We carefully take into account the evolution of the gravitational potential, the source of these induced gravitational waves, during a gradual transition from an early matter-dominated era to the radiation-dominated era, where the transition timescale is comparable to the Hubble time at that time. Realizations of such a gradual transition include the standard perturbative reheating with a constant decay rate. Contrary to previous works, we find that the presence of an early matter-dominated era does not necessarily enhance the induced gravitational waves due to the decay of the gravitational potential around the transition from an early matter-dominated era to the radiation-dominated era.

Contents

1	Introduction	1
2	A formalism to calculate induced gravitational waves	2
3	Evolution of gravitational potential	5
4	Calculations of induced gravitational waves	8
5	Discussion	10

1 Introduction

Stochastic gravitational-wave (GW) background is one of the hottest topics in astrophysics and cosmology. It is generated from numerous astrophysical processes, such as mergers of black holes, neutron stars and white dwarfs (see Ref. [1] and references therein). In addition, there can also be cosmological origins such as vacuum quantum fluctuations during inflation, cosmic strings and scalar perturbations at the second order [2–6] (see also Ref. [7] for a recent review and Ref. [8] for detection prospects). In particular, GWs induced by scalar perturbations at the second order have recently attracted a lot of attention [9–22]. Such induced GWs can be especially important in inflationary scenarios where small-scale primordial fluctuations are enhanced, to the extent that a cosmologically relevant amount of primordial black holes are created by the gravitational collapse of extremely rare peaks during the radiation-dominated (RD) era. In such scenarios, the scalar perturbations may simultaneously induce stochastic GWs that can be detected by current and future GW observations [4, 5, 23, 24]. Even if no sizable amount of primordial black holes was produced, the induced GWs can be used to constrain the amplitude of primordial perturbations on small scales [16, 21]. In this and an accompanying paper [25], we argue that the induced GWs could also be useful probes of an early epoch after inflation and before the RD era.

Throughout this work, we discuss the GWs induced by the scalar (namely curvature/density) perturbations assuming that an early matter-dominated (eMD) era follows inflation, which ends with the Universe dominated by radiation (reheating) [10, 26, 27]. After the inflation era, a massive field, such as the inflaton or a curvaton, could dominate the energy density and the Universe behaves as a matter-dominated (MD) era until the field decays to radiation, which is the beginning of the RD era. Unlike during the RD era, the gravitational potential, which is the source of the induced GWs, does not decay even on subhorizon scales during a MD era. Therefore the presence of an eMD era which precedes the RD era may seem to enhance the induced GWs, relative to the GWs induced from the same primordial spectrum when the transition from inflation to the RD era is virtually instantaneous.

The effects of an eMD era on induced GWs were also discussed in Refs. [10, 26, 27]. In the previous works, they assumed that the gravitational potential is constant on subhorizon scales during an eMD era up to the moment of reheating. However, in realistic situations, the transition from an eMD era to the RD era occurs gradually due to an exponential decay of the massive particle ($\rho_m a^3 \propto \exp(-\Gamma t)$ with Γ denoting its decay rate). As a result,

the gravitational potential also changes gradually. Here, by a gradual-reheating transition we mean that the transition timescale is comparable to the Hubble time at that time. In addition, the authors in the previous works neglected an important part of contributions to the induced GWs associated with the RD era. The part of the contributions mainly comes from the modes that had entered the horizon during an eMD era and have non-negligible impacts on the GW spectrum as we show later. In short, we take into account the gradual evolution of the gravitational potential and calculate GWs induced throughout the transition for the first time.¹ Note that, throughout this paper, we focus on the GWs induced by the perturbations entering the horizon during an eMD era because the effects of an eMD era on induced GWs are mainly due to the behaviors of the perturbations on subhorizon scales during an eMD era, which are different from those during the RD era.

This paper is organized as follows. In Sec. 2, we review the calculations of the induced GWs with some refinements of previous works. The gradual reheating and its consequences, particularly the significant suppression of the gravitational potential, are discussed in Sec. 3. Using the results obtained in these sections, we compute the induced GWs in Sec. 4. Sec. 5 is dedicated to discussions.

2 A formalism to calculate induced gravitational waves

In this section, we introduce formulas to calculate GWs induced around a transition from an eMD era to the RD era. We assume that the curvature perturbations follow a Gaussian distribution.² We take the conformal Newtonian gauge,³ and the metric perturbations are given by

$$ds^2 = a^2 \left(-(1 + 2\Phi)d\eta^2 + \left((1 - 2\Psi)\delta_{ij} + \frac{1}{2}h_{ij} \right) dx^i dx^j \right), \quad (2.1)$$

where $\eta = \int dt/a(t)$ is the cosmic conformal time with a denoting the scale factor. Since we are interested in the second-order contributions to the tensor perturbation h_{ij} originating from the first-order scalar perturbations Φ and Ψ , we neglect the irrelevant components such as the vector perturbations and first-order tensor perturbations. We also neglect anisotropic stress and take $\Psi = \Phi$ in the following. Note that since Φ can be interpreted as the Newtonian potential, Φ is referred to as “gravitational potential”. Throughout this work, we focus on small-scale perturbations with $k \gg k_{\text{eq}} = 0.0103 \text{ Mpc}^{-1}$ [32] and do not take into account the effects associated with the late MD era ($z \lesssim 3400$) [3, 33]. Here, we introduce the formulas only in the case where the transition from an eMD era to the RD era suddenly occurs at a conformal time $\eta = \eta_{\text{R}}$. In Sec. 3, we will explain how to take into account a gradual transition. Since the energy density is continuous at the transition, the scale factor $a = a(\eta)$ and its derivative with respect to the conformal time are also continuous. Then, we can

¹The effects of the decrease in the gravitational potential during a gradual transition and the resultant incomplete enhancement of induced GWs were also discussed in a talk by S. Kuroyanagi [28], though they neglected the difference between the evolutions of the perturbations of matter and radiation. Some qualitative features of our results including the shape of the spectrum Ω_{GW} are somewhat different from theirs.

²GWs induced by scalar perturbations following a non-Gaussian distribution are studied in Refs. [11, 14, 24, 29].

³The gauge dependence of induced GWs is discussed in Refs. [30, 31].

express the scale factor as

$$\frac{a(\eta)}{a(\eta_{\text{R}})} = \begin{cases} \left(\frac{\eta}{\eta_{\text{R}}}\right)^2 & (\eta < \eta_{\text{R}}), \\ 2\frac{\eta}{\eta_{\text{R}}} - 1 & (\eta \geq \eta_{\text{R}}). \end{cases} \quad (2.2)$$

Tensor perturbations can be expanded with the Fourier components as

$$h_{ij}(\eta, \mathbf{x}) = \int \frac{d^3k}{(2\pi)^{3/2}} \left(e_{ij}^+(\mathbf{k}) h_{\mathbf{k}}^+ + e_{ij}^\times(\mathbf{k}) h_{\mathbf{k}}^\times \right) e^{i\mathbf{k}\cdot\mathbf{x}}, \quad (2.3)$$

where e_{ij}^λ ($\lambda : +, \times$) are the polarization tensors. The power spectrum of tensor perturbations is defined as

$$\left\langle h_{\mathbf{k}}^\lambda(\eta) h_{\mathbf{k}'}^{\lambda'}(\eta) \right\rangle = \delta_{\lambda\lambda'} \delta^3(\mathbf{k} + \mathbf{k}') \frac{2\pi^2}{k^3} \mathcal{P}_h(\eta, k), \quad (2.4)$$

where the angle brackets denote an ensemble average. The energy density parameter of GWs per logarithmic interval in k is given by

$$\begin{aligned} \Omega_{\text{GW}}(\eta, k) &= \frac{\rho_{\text{GW}}(\eta, k)}{\rho_{\text{tot}}(\eta)} \\ &= \frac{1}{24} \left(\frac{k}{\mathcal{H}(\eta)} \right)^2 \overline{\mathcal{P}_h(\eta, k)}, \end{aligned} \quad (2.5)$$

where ρ represents the energy density, $\mathcal{H} = a'/a$, with the prime representing derivative with respect to the conformal time, and the overline on the power spectrum indicates the time average over oscillations. The equation of motion of the tensor perturbations is given by [3]

$$h_{\mathbf{k}}^{\lambda''}(\eta) + 2\mathcal{H}h_{\mathbf{k}}^{\lambda'}(\eta) + k^2 h_{\mathbf{k}}^\lambda(\eta) = 4S_{\mathbf{k}}^\lambda(\eta). \quad (2.6)$$

The source term $S_{\mathbf{k}}^\lambda$ is expressed in terms of the Fourier components of the gravitational potential as

$$S_{\mathbf{k}}^\lambda = \int \frac{d^3q}{(2\pi)^{3/2}} e_{ij}^\lambda(\mathbf{k}) q_i q_j \left(2\Phi_{\mathbf{q}} \Phi_{\mathbf{k}-\mathbf{q}} + \frac{4}{3(1+w)} (\mathcal{H}^{-1}\Phi'_{\mathbf{q}} + \Phi_{\mathbf{q}})(\mathcal{H}^{-1}\Phi'_{\mathbf{k}-\mathbf{q}} + \Phi_{\mathbf{k}-\mathbf{q}}) \right), \quad (2.7)$$

where $w = P/\rho$ is the equation-of-state parameter with P being the pressure. Using the Green's function method, we can express the power spectrum of GWs as [10] (see also [2, 3, 23] for detail)

$$\overline{\mathcal{P}_h(\eta, k)} = 4 \int_0^\infty dv \int_{|1-v|}^{1+v} du \left(\frac{4v^2 - (1+v^2 - u^2)^2}{4vu} \right)^2 \overline{I^2(u, v, k, \eta, \eta_{\text{R}})} \mathcal{P}_\zeta(uk) \mathcal{P}_\zeta(vk). \quad (2.8)$$

Here, $\mathcal{P}_\zeta(k)$ is the power spectrum of the primordial curvature perturbations, the integration variables u and v represent wavenumbers in units of k , and the function $I(u, v, k, \eta, \eta_{\text{R}})$ contains information on the dynamics of the scalar and tensor perturbations and is given by

$$I(u, v, k, \eta, \eta_{\text{R}}) = \int_0^x d\bar{x} \frac{a(\bar{\eta})}{a(\eta)} k G_k(\eta, \bar{\eta}) f(u, v, \bar{x}, x_{\text{R}}), \quad (2.9)$$

where x and x_{R} are defined as $x \equiv k\eta$ and $x_{\text{R}} \equiv k\eta_{\text{R}}$. In the above expression, $f(u, v, \bar{x}, x_{\text{R}})$ is the source function defined as

$$f(u, v, \bar{x}, x_{\text{R}}) = \frac{3(2(5+3w)\Phi(u\bar{x})\Phi(v\bar{x}) + 4\mathcal{H}^{-1}(\Phi'(u\bar{x})\Phi(v\bar{x}) + \Phi(u\bar{x})\Phi'(v\bar{x})) + 4\mathcal{H}^{-2}\Phi'(u\bar{x})\Phi'(v\bar{x}))}{25(1+w)}. \quad (2.10)$$

$\Phi(x, x_{\text{R}})$ is the transfer function of the gravitational potential, which satisfies $\Phi(x \rightarrow 0, x_{\text{R}}) = 1$. The second argument of Φ is abbreviated in Eq. (2.10) for compact notation, that is, $\Phi(u\bar{x})$ actually means $\Phi(u\bar{x}, ux_{\text{R}})$ and $\Phi(v\bar{x})$ should be understood similarly. The prime here denotes a differentiation with respect to $\bar{\eta}$. Since a is given in Eq. (2.2), $k\mathcal{H}^{-1}$ can be written as

$$k\mathcal{H}^{-1}(\eta) = \begin{cases} \frac{x}{2} & (\eta < \eta_{\text{R}}), \\ x - \frac{1}{2}x_{\text{R}} & (\eta \geq \eta_{\text{R}}). \end{cases} \quad (2.11)$$

G_k in Eq. (2.9) is the Green's function being the solution of

$$G_k''(\eta, \bar{\eta}) + \left(k^2 - \frac{a''(\eta)}{a(\eta)}\right) G_k(\eta, \bar{\eta}) = \delta(\eta - \bar{\eta}). \quad (2.12)$$

Here, the prime denotes a differentiation with respect to only η , not $\bar{\eta}$. G_k represents the solution for GWs (multiplied by the scale factor) in the presence of a delta-function source.

Ultimately, the time evolutions of all relevant modes for both G_k and Φ need to be calculated for gradual-transition scenarios to obtain induced GWs. Unfortunately, however, we have not been able to find exact analytic solutions of G_k and Φ for such scenarios. In addition, obtaining numerical solutions and plugging them into the formula for the induced GWs to do the relevant integrations require high computational costs. Hence, in this paper, we try to calculate the induced GWs approximately as a first step toward a more rigorous analysis. Let us begin by using Eq. (2.2) to decompose Eq. (2.9) as [10],⁴

$$I(u, v, x, x_{\text{R}}) = \int_0^{x_{\text{R}}} d\bar{x} \left(\frac{1}{2(x/x_{\text{R}}) - 1} \right) \left(\frac{\bar{x}}{x_{\text{R}}} \right)^2 kG_k^{\text{eMD} \rightarrow \text{RD}}(\eta, \bar{\eta}) f(u, v, \bar{x}, x_{\text{R}}) \\ + \int_{x_{\text{R}}}^x d\bar{x} \left(\frac{2(\bar{x}/x_{\text{R}}) - 1}{2(x/x_{\text{R}}) - 1} \right) kG_k^{\text{RD}}(\eta, \bar{\eta}) f(u, v, \bar{x}, x_{\text{R}}) \quad (2.13)$$

$$\equiv I_{\text{eMD}}(u, v, x, x_{\text{R}}) + I_{\text{RD}}(u, v, x, x_{\text{R}}), \quad (2.14)$$

where we have assumed $x > x_{\text{R}}$ (see Eq. (4.3) for $x < x_{\text{R}}$). The first term I_{eMD} represents the contributions from the GWs induced during an eMD era and propagating freely during the RD era. On the other hand, the second term I_{RD} describes the GWs induced during the RD era. The Green's functions G_k for GWs are given by

$$kG_k^{\text{eMD} \rightarrow \text{RD}}(\eta, \bar{\eta}) = C(x, x_{\text{R}})\bar{x}j_1(\bar{x}) + D(x, x_{\text{R}})\bar{x}y_1(\bar{x}), \quad (2.15)$$

and

$$kG_k^{\text{RD}}(\eta, \bar{\eta}) = \sin(x - \bar{x}), \quad (2.16)$$

⁴Eq. (2.13) refines the relevant formula in Ref. [10]. In the limit of $x \rightarrow \infty$, the contribution of the first term to Ω_{GW} decreases by 1/4 compared to the previous result.

where j_1 and y_1 are the first and second spherical Bessel functions, and the coefficients are

$$C(x, x_R) = \frac{\sin x - 2x_R(\cos x + x_R \sin x) + \sin(x - 2x_R)}{2x_R^2}, \quad (2.17)$$

and

$$D(x, x_R) = \frac{(2x_R^2 - 1) \cos x - 2x_R \sin x + \cos(x - 2x_R)}{2x_R^2}. \quad (2.18)$$

Note that when we derive C and D , we have connected the GW solutions at the transition requiring continuity of themselves and also their first derivatives [10].

As we can see from Eqs. (2.10) and (2.13), the induced GWs sensitively depend on the evolution of the gravitational potential Φ . In Refs. [26, 27], they assume that Φ remains unity until η_R and that I_{RD} , representing the contributions from the RD era, is subdominant and hence can be neglected. However, as we will see in the next section, Φ gradually changes around the transition and therefore we need to take into account the evolution of Φ more carefully. The contributions from the RD era also turn out to have non-negligible impacts. These are the main issues we address in this work.

From the above splitting of the function I , we have

$$\overline{I^2(u, v, x, x_R)} = \overline{I_{\text{eMD}}^2(u, v, x, x_R)} + \overline{I_{\text{RD}}^2(u, v, x, x_R)} + 2\overline{I_{\text{RD}}I_{\text{eMD}}(u, v, x, x_R)}. \quad (2.19)$$

For later convenience, we also split Ω_{GW} into three parts as $\Omega_{\text{GW}} = \Omega_{\text{GW, RD}} + \Omega_{\text{GW, eMD}} + \Omega_{\text{GW, cross}}$, where $\Omega_{\text{GW, RD}}$, $\Omega_{\text{GW, eMD}}$, and $\Omega_{\text{GW, cross}}$ are calculated from $\overline{I_{\text{RD}}^2}$, $\overline{I_{\text{eMD}}^2}$ and $2\overline{I_{\text{RD}}I_{\text{eMD}}}$, respectively. Note that $\Omega_{\text{GW, cross}}$ can be negative.

After the transition, the gravitational potential continues to decay on subhorizon scales and Ω_{GW} reaches some constant value. Hence, we define η_c as the moment when Ω_{GW} stops growing. Since we consider small-scale perturbations, η_c is well before the late matter-radiation equality time.

3 Evolution of gravitational potential

In this section, we focus on the evolution of Φ around the transition, which has large impacts on the resultant GWs. To be concrete, we assume that the field that dominates the Universe during an eMD era, such as inflaton, decays to radiation with a constant decay rate Γ . In this case, we can use formulas for perturbations in decaying dark matter scenarios [34–36].⁵ Then, the evolutions of the energy densities are described by [36]

$$\rho'_m = -(3\mathcal{H} + a\Gamma)\rho_m, \quad (3.1)$$

$$\rho'_r = -4\mathcal{H}\rho_r + a\Gamma\rho_m, \quad (3.2)$$

⁵Strictly speaking, the perturbations of the coherently oscillating scalar field behave differently from the dust-like fluid for $k \gtrsim \sqrt{am\mathcal{H}}$ (m : mass of the oscillating field) (see Ref. [37] and references therein). However, for the perturbations that enter the horizon during an eMD era, which we focus on in this paper, we can regard the fluid of the oscillating field as a dust-like fluid (even for the perturbations of the oscillating field). The reason is as follows. The comoving horizon scale at the beginning of the eMD era is given as $\sim (am)^{-1}$ at that time because the inflaton or curvaton starts to oscillate and the eMD era begins when $\mathcal{H} \sim am$. Then, the wavenumber of the perturbation entering the horizon during the eMD era satisfies $k < ma|_{t=t_{\text{eMD, start}}} < \sqrt{am\mathcal{H}}$ ($t_{\text{eMD, start}}$: the start time of the eMD era), considering the fact that $\sqrt{am\mathcal{H}}$ is proportional to $a^{1/4}$ during the eMD era. Therefore, we regard the fluid of the oscillating field as a dust-like fluid throughout this paper.

where the subscripts “m” and “r” represent matter and radiation, respectively. The equations for perturbations in Fourier space are given by [36]

$$\delta'_m = -\theta_m + 3\Phi' - a\Gamma\Phi, \quad (3.3)$$

$$\theta'_m = -\mathcal{H}\theta_m + k^2\Phi, \quad (3.4)$$

$$\delta'_r = -\frac{4}{3}(\theta_r - 3\Phi') + a\Gamma\frac{\rho_m}{\rho_r}(\delta_m - \delta_r + \Phi), \quad (3.5)$$

$$\theta'_r = \frac{k^2}{4}\delta_r + k^2\Phi - a\Gamma\frac{3\rho_m}{4\rho_r}\left(\frac{4}{3}\theta_r - \theta_m\right), \quad (3.6)$$

where δ and θ denote the energy density perturbation and the velocity divergence [36, 38], respectively, and we have neglected the anisotropic stress of radiation. In addition, the derivative of Φ is given by [39],

$$\Phi' = -\frac{k^2\Phi + 3\mathcal{H}^2\Phi + \frac{3}{2}\mathcal{H}^2\left(\frac{\rho_m}{\rho_{\text{tot}}}\delta_m + \frac{\rho_r}{\rho_{\text{tot}}}\delta_r\right)}{3\mathcal{H}}, \quad (3.7)$$

where $\rho_{\text{tot}} = \rho_m + \rho_r$.

Figure 1 shows the numerical results for the evolutions of the background quantities, such as a , ρ_m , ρ_r , and w . We define η_{eq} as the conformal time when $\rho_m = \rho_r$. Note that there is one-to-one correspondence between Γ and η_{eq} and hence this and the subsequent figures do not depend on the specific choice of Γ . We also plot the approximation formula Eq. (2.2) with $\eta_{\text{R}} = 0.83\eta_{\text{eq}}$, as well as the following fitting formula:

$$w_{\text{fit}} = \frac{1}{3}\left(1 - \exp\left(-0.7\left(\frac{\eta}{\eta_{\text{eq}}}\right)^3\right)\right). \quad (3.8)$$

Both the formulas fit the numerical results very well. We will explain the reason why we take $\eta_{\text{R}} = 0.83\eta_{\text{eq}}$ shortly. The fact that the approximation formula for the scale factor fits the numerical result well may indicate that using the exact solutions for the Green’s functions during an eMD era and the RD era is a good approximation, noting the Green’s functions are determined by the scale factor (see Eq. (2.12)).

Figure 2 shows the numerical results of the evolutions of the perturbations. Here, we have assumed the following adiabatic initial conditions [39]:⁶

$$\delta_{m,\text{ini}} = -2\Phi_{\text{ini}}, \quad \delta_{r,\text{ini}} = \frac{4}{3}\delta_{m,\text{ini}}, \quad \theta_{m,\text{ini}} = \theta_{r,\text{ini}} = \frac{k^2\eta}{3}\Phi_{\text{ini}}. \quad (3.9)$$

Note that we study the linear regime, and thus the overall normalization of perturbations does not matter in the figures, hence we take $\Phi_{\text{ini}} = 1$, or equivalently we plot the transfer function. In Fig. 2, we can see that for perturbation modes that entered the horizon well before the transition ($k \gg 1/\eta_{\text{eq}}$), the gravitational potential Φ exponentially decays soon after the equality time, and after a while, Φ starts to oscillate due to radiation pressure, with the amplitude decaying less rapidly ($\propto \eta^{-2}$).

Here, we explain how to derive an approximation formula of Φ which describes its exponential decay. The formula will be used to calculate the induced GWs. First, from

⁶Strictly speaking, in Ref. [39], the initial conditions for $\theta_{m/r}$ are not discussed. However, we can easily derive the initial conditions for them substituting the initial condition for δ_m into Eq. (3.4).

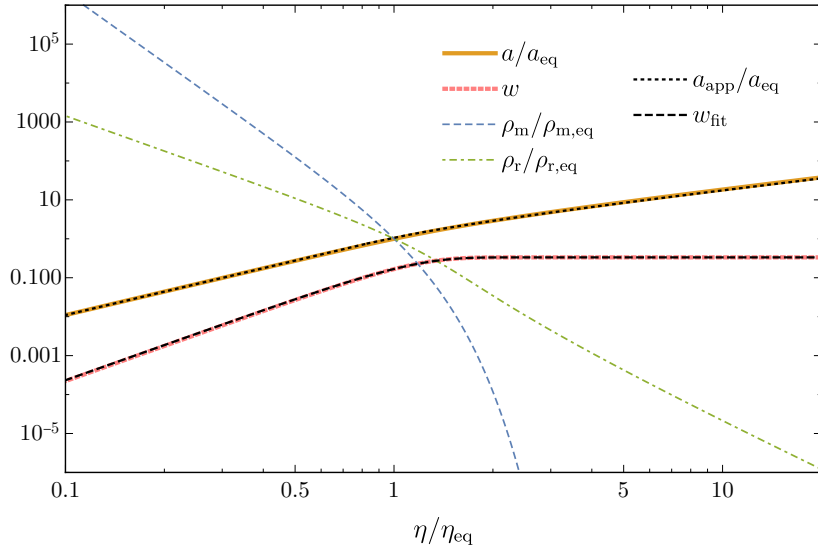


Figure 1: Time dependences of the scale factor, the energy densities, normalized by their values at $\eta = \eta_{\text{eq}}$, and the equation-of-state parameter. a_{app} is given by Eq. (2.2) with $\eta_{\text{R}} = 0.83\eta_{\text{eq}}$ and w_{fit} is given by Eq. (3.8). Note that $\rho_{\text{m,eq}} = \rho_{\text{r,eq}}$ by definition.

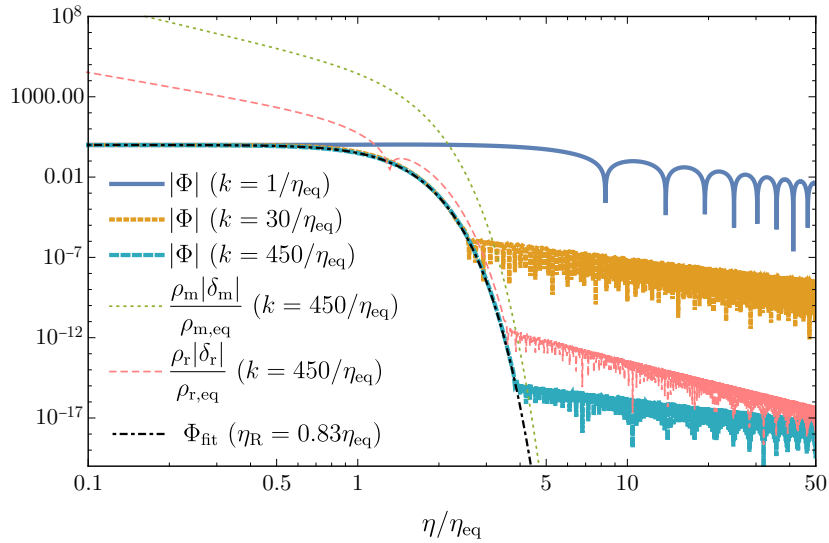


Figure 2: Time dependences of the gravitational potential and the energy density perturbations. Φ_{fit} is given by Eq. (3.10).

Eq. (3.7), Φ can be approximated to be $k^2\Phi \simeq \frac{3}{2}\mathcal{H}^2 \left(\frac{\rho_{\text{m}}}{\rho_{\text{tot}}}\delta_{\text{m}} + \frac{\rho_{\text{r}}}{\rho_{\text{tot}}}\delta_{\text{r}} \right)$ in the subhorizon limit. For modes with $k \gg 1/\eta_{\text{eq}}$, during $1/k \ll \eta \ll \eta_{\text{eq}}$, δ_{m} grows but δ_{r} does not. Therefore, even after η_{eq} , the evolution of Φ is dominated by $\rho_{\text{m}}\delta_{\text{m}}$ for a while. During this phase, ρ_{m} decays exponentially and then we can expect Φ is proportional to ρ_{m} . Radiation density perturbations $\rho_{\text{r}}\delta_{\text{r}}$ also decay following the decay of Φ around this phase. After a while, the evolution of Φ is dominated by $\rho_{\text{r}}\delta_{\text{r}}$ and then Φ starts to oscillate. Neglecting this

radiation term and the expansion of the Universe during the transition for simplicity, we can approximate Φ as

$$\begin{aligned}\Phi &\sim \exp\left(-\int^{\eta} d\bar{\eta} a(\bar{\eta})\Gamma\right) \\ &= \begin{cases} \exp\left(-\frac{2}{3}\left(\frac{\eta}{\eta_R}\right)^3\right) & (\eta < \eta_R), \\ \exp\left(-2\left(\left(\frac{\eta}{\eta_R}\right)^2 - \frac{\eta}{\eta_R} + \frac{1}{3}\right)\right) & (\eta \geq \eta_R), \end{cases} \\ &\equiv \Phi_{\text{fit}},\end{aligned}\tag{3.10}$$

where we have used Eq. (2.2) and assumed $a(\eta_R)\Gamma = \mathcal{H}(\eta_R)(= 2/\eta_R)$. Note that since we consider a gradual decay of the dominant field, there is some ambiguity in the definition of η_R , and hence we may choose values of η_R which are slightly different from η_{eq} . From Fig. 2, we can see that if we take $\eta_R = 0.83\eta_{\text{eq}}$, the approximation formula fits the non-oscillating part of the numerical results very well. As we have seen in Fig. 1, the approximation formula of the scale factor, given by Eq. (2.2) with $\eta_R = 0.83\eta_{\text{eq}}$, also fits the numerical result very well. Therefore we take $\eta_R = 0.83\eta_{\text{eq}}$ when we use Eqs. (2.2) and (3.10) in the following. Figure 3 is an enlarged view of the evolution of Φ for several modes around the transition. From this figure, we can see that, for $k \gtrsim 30/\eta_{\text{eq}}$, the exponential decay of Φ can be fitted by Eq. (3.10).

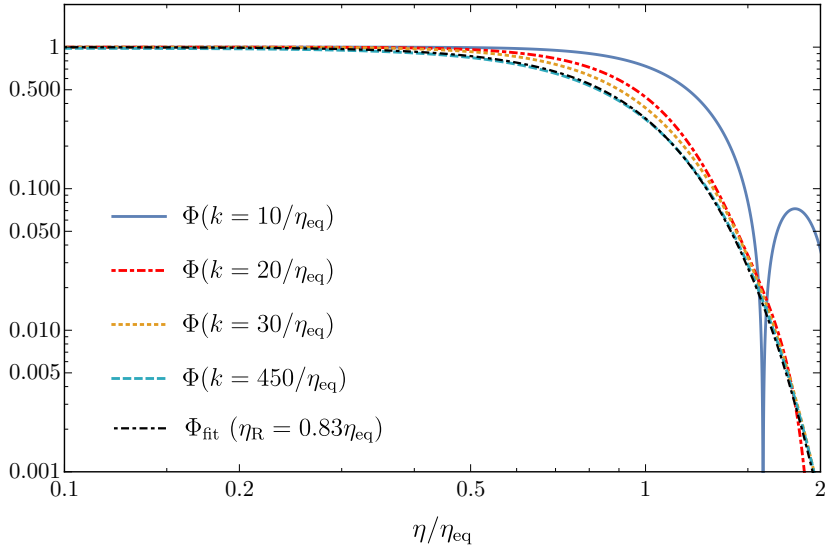


Figure 3: Evolutions of Φ with different wave numbers ($10/\eta_{\text{eq}} \leq k \leq 450/\eta_{\text{eq}}$) and the fitting formula [Eq. (3.10)].

4 Calculations of induced gravitational waves

In this section, we explain how we approximately calculate induced GWs in gradual-transition scenarios and present the results. We consider the power spectrum given by

$$\mathcal{P}_\zeta = A \Theta(k - 30/\eta_{\text{eq}}) \Theta(k_{\text{max}} - k),\tag{4.1}$$

where A represents the amplitude. We focus on modes with $k > 30/\eta_{\text{eq}}$ so that we can use the fitting formula for Φ obtained in the previous section. In addition, we have introduced the cutoff scale k_{max} . This cutoff scale corresponds to the horizon scale at the start of an eMD era, or the scale that is entering the non-linear regime at η_{R} , i.e., the amplitude of matter density perturbations on such a scale becomes unity at η_{R} . Since the formulas shown above are invalid in the non-linear regime, we need to introduce this cutoff scale to limit our analysis to the linear regime when there exist scales that enter the non-linear regime before η_{R} . The scale corresponding to the non-linear growth of the perturbations is roughly estimated as [10, 26]

$$k_{\text{NL}} \sim \sqrt{\frac{5}{2}} \mathcal{P}_{\zeta}^{-1/4} \mathcal{H}(\eta_{\text{R}}) \sim 470/\eta_{\text{R}}. \quad (4.2)$$

Therefore our calculations are valid only for $k_{\text{max}} \lesssim 470/\eta_{\text{R}}$. To make the differences from the previous works look clear, we take $k_{\text{max}} = 450/\eta_{\text{R}}$ in the following.

With the above power spectrum, we can use the fitting formula of Φ , given in Eq. (3.10). As we have seen in Sec. 3, the expression of the scale factor for a sudden transition, given in Eq. (2.2), describes the numerical results very well, and this justifies the use of the formulas for the induced GWs, introduced in Sec. 2 with the separation of the contributions at η_{R} . Then, to calculate induced GWs, we substitute the fitting formulas of w and Φ for a gradual transition, given in Eqs. (3.8) and (3.10), into Eq. (2.10), thereby taking into account the graduality of the transition. Note that we neglect contributions from the oscillation phases of Φ because the oscillation amplitude is very small for $k > 30/\eta_{\text{eq}}$, noting that the power spectrum of the induced GWs is basically proportional to the fourth power of Φ . For example, in Fig. 2, we can see that Φ with $k = 30/\eta_{\text{eq}}$ starts to oscillate with the amplitude $\Phi \sim \mathcal{O}(10^{-6})$.

Figure 4 shows the numerical results for the induced GWs. From this figure, we can see that the induced GWs (thick black solid line) are suppressed compared to those derived with the setups in the previous works (brown dotted line). In this figure, each component of the induced GWs is also shown (blue solid, blue dotted, and blue dashed/red dot-dashed lines for $\Omega_{\text{GW,eMD}}$, $\Omega_{\text{GW,RD}}$, and $\pm\Omega_{\text{GW,cross}}$, respectively). From these plots, we understand two reasons for the suppression. First, each component of the induced GWs is suppressed because Φ is smaller than unity around the transition, as we have seen in the previous section. The second reason is that a cancellation occurs between those components. (Note again that $\Omega_{\text{GW,cross}}$ can be negative by definition.)

To see how the cancellation arises, we show the time dependence of $x|I|$ in Fig. 5. For $\eta > \eta_{\text{R}}$, we use Eq. (2.13) and, for $\eta < \eta_{\text{R}}$, we use

$$I(u, v, x, x_{\text{R}}) = \int_0^x d\bar{x} \left(\frac{\bar{x}}{x}\right)^2 kG_k^{\text{eMD}}(\eta, \bar{\eta}) f(v, u, \bar{x}, x_{\text{R}}), \quad (4.3)$$

which can be derived from Eq. (2.9), with kG_k^{eMD} given by [3, 26]

$$kG_k^{\text{eMD}}(\eta, \bar{\eta}) = -x\bar{x}(j_1(x)y_1(\bar{x}) - y_1(x)j_1(\bar{x})). \quad (4.4)$$

From Fig. 5, we can see that xI grows when $\eta \ll \eta_{\text{R}}$, but around the transition ($\eta \sim \eta_{\text{R}}$), xI stops growing and starts to decrease due to the decay of Φ . This again shows the cancellation between I_{eMD} and I_{RD} . After the transition ($\eta > \mathcal{O}(1)\eta_{\text{R}}$), xI oscillates with its amplitude being almost constant. Since the evolutions of I correspond to those of the tensor

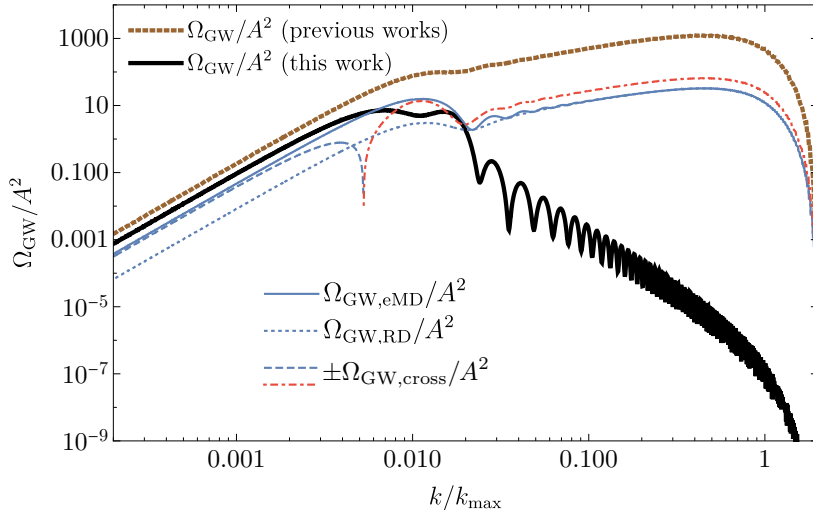


Figure 4: Spectrum of induced GWs at $\eta = \eta_c$ associated with a gradual transition from an eMD era to the RD era. For all the plots, $k_{\max} = 450/\eta_R$ is assumed and the primordial power spectrum used is given in Eq. (4.1). Our results for Ω_{GW} are shown by the thick black solid line. It is the sum of each component: $\Omega_{\text{GW,eMD}}$ (blue solid), $\Omega_{\text{GW,RD}}$ (blue dotted), and $\pm\Omega_{\text{GW,cross}}$ (blue dashed/red dot-dashed). The thick brown dotted line shows the result using Ref. [10], additionally taking into account the factor 1/4 mentioned in footnote 4, with the same assumptions as in Refs. [26], under which $\Phi = 1$ until $\eta = \eta_R$ ($I_{\text{RD}} = 0$). Reduction from the brown dotted line to the black solid line shows the effects of the gradual transition.

perturbations, the behavior of xI can be interpreted as follows. During an eMD era, since the source term in Eq. (2.6) is almost constant, the amplitude of the tensor perturbation is given as $h_{\mathbf{k}}^\lambda \simeq 4S_{\mathbf{k}}^\lambda/k^2$ in the subhorizon limit [3, 26]. Here, we consider a gradual transition from an eMD era to the RD era and therefore the amplitude of the tensor perturbations decays on subhorizon scales, following the gradual decay of the source during the transition, which corresponds to the decay of xI around $\eta \sim \eta_R$. After a while, the tensor perturbations decouple from the source and behave as freely propagating GWs, which corresponds to the oscillation of xI for $\eta > \mathcal{O}(1)\eta_R$.

Note that, also to obtain Fig. 5, we use the approximation formula Φ_{fit} for Φ and neglect the oscillation behavior of Φ after its exponential decay. This also implies that the oscillation behavior of xI in Fig. 5 (already present before $\eta = 2.5\eta_{\text{eq}} \simeq 3.0\eta_R$) has nothing to do with the oscillation behavior of Φ in Fig. 2 (appearing after $\eta = 2.5\eta_{\text{eq}}$ in $k > 30/\eta_{\text{eq}}$), and the contributions from the oscillations of Φ can be neglected because of its small amplitude if we consider $k > 30/\eta_{\text{eq}}$, as we have already mentioned.

5 Discussion

In this paper, we have revisited the effects of an eMD era on the GWs induced by the scalar perturbations. We have considered a case where the energy density in the eMD era is dominated by the field decaying to radiation with a constant decay rate, which leads to a gradual transition to the RD era. We have taken into account the evolution of the gravitational potential Φ during the transition and found that the existence of an eMD era

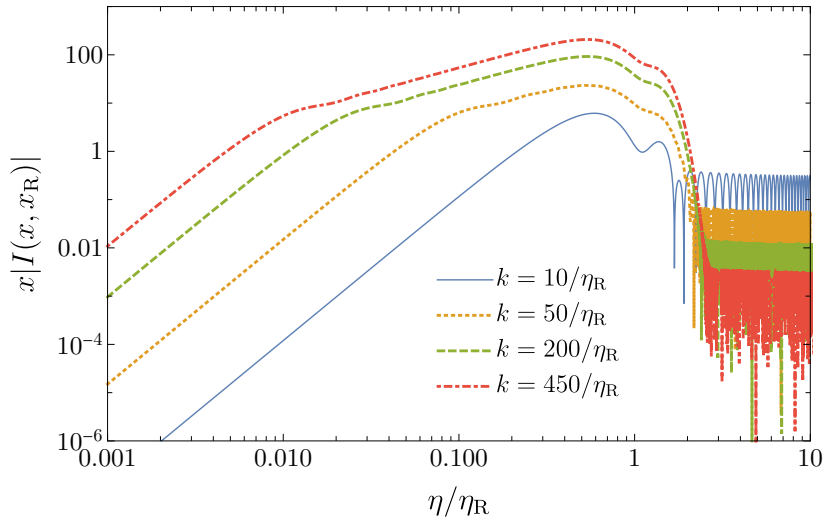


Figure 5: Time dependences of $x|I(x, x_R)|$, defined in Eq. (2.9). We omit the arguments u and v because we approximate Φ as Φ_{fit} , defined in Eq. (3.10), and hence I does not depend on u or v .

does not necessarily increase the induced GWs as were reported in previous works. This is due to the exponential decay of Φ during the transition.

Throughout this work, to spotlight the effects of an eMD era on induced GWs, we have focused on the GWs induced by the perturbations entering the horizon during an eMD era. However, we have neglected the contributions from the perturbations entering the horizon during an eMD era but relatively near the transition ($1/\eta_R < k < 30/\eta_{\text{eq}}$) to avoid high computational costs. If we consider the scale-invariant spectrum of curvature perturbations, these perturbations could produce GWs in addition to the results in Fig. 4. We leave the analysis of these additional effects of an eMD era for our future work in a separate paper. In addition, we have not considered the GWs induced by the perturbations entering the horizon much before the transition ($k > 470/\eta_R$). If we consider the scale-invariant spectrum and a long-lasting eMD era, the perturbations on $k > 470/\eta_R$ could also induce additional GWs. Such perturbations may have become non-linear during the eMD era, and our formula based on the linear perturbation theory cannot be applied. Although there are works discussing GWs induced by non-linear scalar perturbations in this context [40, 41], there are still some uncertainties about the predictions [40, 41]. Therefore, the amount of the induced GWs predicted in the current work can be regarded as lower bounds on the total induced GWs.

Although we assume that the decay rate is constant throughout this paper, if we consider a time-dependent decay rate causing the field to decay much faster than the Hubble time at that time, the induced GWs can be significantly enhanced. We discuss this issue in Ref. [25].

Acknowledgments

The authors thank Matthew Pearce, Csaba Balazs, Lauren Pearce, and Graham White for pointing out the error in Figs. 4 and 5 in the previous version of this paper. KK and TT thank Sachiko Kuroyanagi for useful discussions. KI acknowledges Misao Sasaki, Tomohiro Fujita, Teruaki Suyama, and Masahide Yamaguchi for useful comments. KI and TN are

grateful to KEK or hospitality received during this work. This work was supported in part by World Premier International Research Center Initiative (WPI Initiative), MEXT, Japan, the JSPS Research Fellowship for Young Scientists (KI and TT), JSPS KAKENHI Grants No. JP18J12728 (KI), No. JP17H01131 (KK), and No. JP17J00731 (TT), MEXT KAKENHI Grants No. JP15H05889 (KK), No. JP18H04594 (KK) and No. JP19H05114 (KK), and Advanced Leading Graduate Course for Photon Science (KI).

References

- [1] Nelson Christensen. Stochastic Gravitational Wave Backgrounds. Rept. Prog. Phys., 82(1):016903, 2019.
- [2] Kishore N. Ananda, Chris Clarkson, and David Wands. The Cosmological gravitational wave background from primordial density perturbations. Phys. Rev., D75:123518, 2007.
- [3] Daniel Baumann, Paul J. Steinhardt, Keitaro Takahashi, and Kiyotomo Ichiki. Gravitational Wave Spectrum Induced by Primordial Scalar Perturbations. Phys. Rev., D76:084019, 2007.
- [4] Ryo Saito and Jun’ichi Yokoyama. Gravitational wave background as a probe of the primordial black hole abundance. Phys. Rev. Lett., 102:161101, 2009. [Erratum: Phys. Rev. Lett.107,069901(2011)].
- [5] Ryo Saito and Jun’ichi Yokoyama. Gravitational-Wave Constraints on the Abundance of Primordial Black Holes. Prog. Theor. Phys., 123:867–886, 2010. [Erratum: Prog. Theor. Phys.126,351(2011)].
- [6] Laila Alabidi, Kazunori Kohri, Misao Sasaki, and Yuuiti Sendouda. Observable Spectra of Induced Gravitational Waves from Inflation. JCAP, 1209:017, 2012.
- [7] Chiara Caprini and Daniel G. Figueroa. Cosmological Backgrounds of Gravitational Waves. Class. Quant. Grav., 35(16):163001, 2018.
- [8] Sachiko Kuroyanagi, Takeshi Chiba, and Tomo Takahashi. Probing the Universe through the Stochastic Gravitational Wave Background. JCAP, 1811(11):038, 2018.
- [9] José Ramón Espinosa, Davide Racco, and Antonio Riotto. A Cosmological Signature of the SM Higgs Instability: Gravitational Waves. JCAP, 1809(09):012, 2018.
- [10] Kazunori Kohri and Takahiro Terada. Semianalytic calculation of gravitational wave spectrum nonlinearly induced from primordial curvature perturbations. Phys. Rev., D97(12):123532, 2018.
- [11] Rong-gen Cai, Shi Pi, and Misao Sasaki. Gravitational Waves Induced by non-Gaussian Scalar Perturbations. 2018.
- [12] N. Bartolo, V. De Luca, G. Franciolini, M. Peloso, and A. Riotto. The Primordial Black Hole Dark Matter - LISA Serendipity. 2018.
- [13] N. Bartolo, V. De Luca, G. Franciolini, M. Peloso, D. Racco, and A. Riotto. Testing Primordial Black Holes as Dark Matter through LISA. 2018.
- [14] Caner Unal. Imprints of Primordial Non-Gaussianity on Gravitational Wave Spectrum. Phys. Rev., D99(4):041301, 2019.
- [15] Christian T. Byrnes, Philippa S. Cole, and Subodh P. Patil. Steepest growth of the power spectrum and primordial black holes. 2018.
- [16] Keisuke Inomata and Tomohiro Nakama. Gravitational waves induced by scalar perturbations as probes of the small-scale primordial spectrum. Phys. Rev., D99(4):043511, 2019.
- [17] Sebastien Clesse, Juan García-Bellido, and Stefano Orani. Detecting the Stochastic Gravitational Wave Background from Primordial Black Hole Formation. 2018.

- [18] Rong-Gen Cai, Shi Pi, Shao-Jiang Wang, and Xing-Yu Yang. Resonant multiple peaks in the induced gravitational waves. 2019.
- [19] Yi-Fu Cai, Chao Chen, Xi Tong, Dong-Gang Wang, and Sheng-Feng Yan. When Primordial Black Holes from Sound Speed Resonance Meet a Stochastic Background of Gravitational Waves. 2019.
- [20] Sai Wang, Takahiro Terada, and Kazunori Kohri. Prospective constraints on the primordial black hole abundance from the stochastic gravitational-wave backgrounds produced by coalescing events and curvature perturbations. 2019.
- [21] Ido Ben-Dayan, Brian Keating, David Leon, and Ira Wolfson. Constraints on Scalar and Tensor spectra from N_{eff} . 2019.
- [22] Yuichiro Tada and Shuichiro Yokoyama. Primordial black hole tower: Dark matter, earth-mass, and LIGO black holes. 2019.
- [23] Keisuke Inomata, Masahiro Kawasaki, Kyohei Mukaida, Yuichiro Tada, and Tsutomu T. Yanagida. Inflationary primordial black holes for the LIGO gravitational wave events and pulsar timing array experiments. *Phys. Rev.*, D95(12):123510, 2017.
- [24] Juan Garcia-Bellido, Marco Peloso, and Caner Unal. Gravitational Wave signatures of inflationary models from Primordial Black Hole Dark Matter. *JCAP*, 1709(09):013, 2017.
- [25] Keisuke Inomata, Kazunori Kohri, Tomohiro Nakama, and Takahiro Terada. Enhancement of Gravitational Waves Induced by Scalar Perturbations due to a Sudden Transition from an Early Matter Era to the Radiation Era. 2019.
- [26] Hooshyar Assadullahi and David Wands. Gravitational waves from an early matter era. *Phys. Rev.*, D79:083511, 2009.
- [27] Laila Alabidi, Kazunori Kohri, Misao Sasaki, and Yuuiti Sendouda. Observable induced gravitational waves from an early matter phase. *JCAP*, 1305:033, 2013.
- [28] Sachiko Kuroyanagi. Gravitational waves from 2nd order scalar perturbations. a talk in the 2nd LeCosPA Symposium, December, 2015.
- [29] Tomohiro Nakama, Joseph Silk, and Marc Kamionkowski. Stochastic gravitational waves associated with the formation of primordial black holes. *Phys. Rev.*, D95(4):043511, 2017.
- [30] Jai-Chan Hwang, Donghui Jeong, and Hyerim Noh. Gauge dependence of gravitational waves generated from scalar perturbations. *Astrophys. J.*, 842(1):46, 2017.
- [31] Frederico Arroja, Hooshyar Assadullahi, Kazuya Koyama, and David Wands. Cosmological matching conditions for gravitational waves at second order. *Phys. Rev.*, D80:123526, 2009.
- [32] N. Aghanim et al. Planck 2018 results. VI. Cosmological parameters. 2018.
- [33] Silvia Mollerach, Diego Harari, and Sabino Matarrese. CMB polarization from secondary vector and tensor modes. *Phys. Rev.*, D69:063002, 2004.
- [34] Kiyotomo Ichiki, Masamune Oguri, and Keitaro Takahashi. WMAP constraints on decaying cold dark matter. *Phys. Rev. Lett.*, 93:071302, 2004.
- [35] Benjamin Audren, Julien Lesgourgues, Gianpiero Mangano, Pasquale Dario Serpico, and Thomas Tram. Strongest model-independent bound on the lifetime of Dark Matter. *JCAP*, 1412(12):028, 2014.
- [36] Vivian Poulin, Pasquale D. Serpico, and Julien Lesgourgues. A fresh look at linear cosmological constraints on a decaying dark matter component. *JCAP*, 1608(08):036, 2016.
- [37] J. A. R. Cembranos, A. L. Maroto, and S. J. Núñez Jareño. Cosmological perturbations in coherent oscillating scalar field models. *JHEP*, 03:013, 2016.

- [38] Chung-Pei Ma and Edmund Bertschinger. Cosmological perturbation theory in the synchronous and conformal Newtonian gauges. *Astrophys. J.*, 455:7–25, 1995.
- [39] Viatcheslav Mukhanov. *Physical Foundations of Cosmology*. Cambridge Univ. Press, Cambridge, 2005.
- [40] Karsten Jedamzik, Martin Lemoine, and Jerome Martin. Collapse of Small-Scale Density Perturbations during Preheating in Single Field Inflation. *JCAP*, 1009:034, 2010.
- [41] Karsten Jedamzik, Martin Lemoine, and Jerome Martin. Generation of gravitational waves during early structure formation between cosmic inflation and reheating. *JCAP*, 1004:021, 2010.